Keyou Chen, Feng Feng, Jonas Kleiner, and Daniel Flamm "Customized non-diffracting beams for advanced transparent materials processing", Proc. SPIE 11991, Frontiers in Ultrafast Optics: Biomedical, Scientific, and Industrial Applications XXII, 1199108 (4 March 2022); https://doi.org/10.1117/12.2609233.

Customized non-diffracting beams for advanced transparent materials processing

Keyou Chen,[a] Feng Feng,[a] Jonas Kleiner,[b] and Daniel Flamm[b]

[a]TRUMPF China Co., Ltd. No. 68, Nanjing East Road, 215400 Taicang, China
[b]TRUMPF Laser- und Systemtechnik GmbH, Johann-Maus-Str. 2, 71254 Ditzingen, Germany

ABSTRACT

We report on the design and realization of novel non-diffracting beams for ultrashort laser materials processing. Our method is axicon based and introduces subtle azimuthal modifications to the conical lenses or well-defined misalignments to achieve a set of novel non-diffracting beams. These focus distributions retain all well-known advantages of non-diffracting beams, such as self-healing, high optical efficiency, or possible extreme aspect ratios. Additionally, tailored transverse intensity profiles with, for example, well-defined preferential direction can be generated. Clear advantages for controlling residual stress and crack orientation in glass processing are discussed and results of different micro-machining experiments are presented.

Keywords: Beam shaping, ultrafast optics, laser materials processing, digital holography, structured light, transparent materials, non-diffracting beams, axicons

1. INTRODUCTION

The class of non-diffracting beams with the Bessel-Gaussian beam as its most famous representative,[1,2] today, is often used for efficient and robust micro-machining using ultrashort laser pulses.[3–7] Several salient features[1,2,8] such as, e.g., the self-healing property or possible extreme aspect ratios enable robust and precise volume machining ranging from cutting to drilling to welding.[6,9] The single-pass, full-thickness cleaving of cm-thick transparent materials using asymmetric Bessel-like for controlling cracks impressively demonstrated the potential of using adapted non-diffracting beams for advanced micro machining.[7,10]

The paper will present several simple and robust optical concepts for further degrees of freedom in shaping customized non-diffracting beams. By using so-called generalized axicons—conical lenses with arbitrary azimuthal dependencies[11]—non-diffracting beams with tailored transverse intensity profiles can be generated. The resulting focus distributions show clear advantages for controlling the residual stress distribution around type-III-regime glass modifications[12] relevant for, e.g., efficient selective laser etching.[13] A second, related, structured light concept makes use of standard axicons and controlled misalignments. The resulting non-diffracting focus distribution exhibits a clear elliptical on-axis intensity maximum where both orientation and main axis ratio can be precisely controlled. We will discuss the beneficial use of this blade-like focus distribution for ultrafast laser materials processing and present experimental results for cutting and etching of transparent materials.

2. GENERALIZED AXICON-BASED GENERATION

Recently, we have introduced the concept of using "generalized axicons" to shape non-diffracting beams with tailored transverse field properties, see Ref. 11. Mentioned modified axicon lenses still exhibit constant slopes in radial direction but can take arbitrary azimuthal dependencies.[11,14] Starting with J. Durnin's description using scalar diffraction theory,[15] an optical field $E(x, y, z)$ has to full fill the following relations to show non-diffracting properties

$$E(x,y,z) = \int_{-\pi}^{\pi} C(\tau) \exp\left(ik_x x + ik_y y + ik_z z\right) d\tau \qquad (1)$$

Further author information:
E-Mail: keyou.chen@trumpf.com.

Proc. SPIE 11991, Frontiers in Ultrafast Optics: Biomedical, Scientific, and Industrial Applications XXII © 2022 SPIE.
https://doi.org/10.1117/12.2609233.

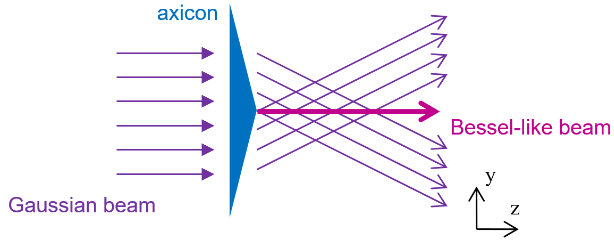

Figure 1. Ray optical representation of the basic optical setup for generating Bessel-like beams with axicons (near-field generation).[1,14] Particularly beneficial is to embed the axicon (or axicon-like element) in two telescopes[18] in order to flexibly adapt the spatial characteristics (length and diameter of the central on-axis maximum) of the non-diffracting beam to the workpiece.[19]

with the wave vector k defined by the laser's wavelength λ

$$k^2 = k_r^2 + k_z^2 = \left(\frac{2\pi}{\lambda}\right)^2 \tag{2}$$

and corresponding components

$$k_x = k_r \sin\tau \qquad k_y = k_r \cos\tau \tag{3}$$

$$k_r^2 = k_x^2 + k_y^2 = \text{const.} \qquad k_z = \text{const.} \tag{4}$$

In fact, Eqs. (1)–(3) represent the computational model of angular spectrum method[16] and are valid for general case. If Eq. (4) is fulfilled by the optical field a non-diffracting beam is at hand.

A widely-used realization method for zeroth-order Bessel beam, a well-known non-diffracting beam, is illuminating the axicon with collimated Gaussian beam,[17] Fig. 1. Please note that the generated Bessel beam has limited size unlike the theoretical case and it is called Bessel-like beam or Gaussian-Bessel beam.

The equivalent phase mask of an axicon under "thin element approximation"[20] in polar coordinate can be written as $\Phi_{\text{axicon}}(\theta, r) = k_r r + C$, depicted in Fig. 2.(b),[21] θ is the azimuthal angle, k_r is the radial frequency of the structure, r is the radius, C is arbitrary constant. Base on this relation, we propose a simple and versatile equation[11,14]

$$\Phi_{\text{mask}}(\theta, r) = k_r r + \phi(\theta), \tag{5}$$

where $\phi(\theta)$ corresponds to the phase of plane wave in Eq. (1), or the phase of the angular spectrum. For interpretation, we refer to Ref. 11 and angular spectrum method.[16] Note, that following our strategy, there is no amplitude modulation, so the term $C(\tau)$ in Eq. (1) is constant. With this equation and simple side conditions, the design of customized non-diffracting beam is significantly accelerated. For example, it is practical to divide the phase mask into 200 fan-sections, which corresponds to 200 plane waves with same number of azimuthal propagation angles.[11] Then the task is to find the best configuration of 200 phase absolute values to define $\phi(\theta)$. For special high-symmetry design tasks the number of fan-sections can be reduced even to 50.[11] From our experience suitable optimization results can easily be achieved and even the simplest optimization procedure, "try and error", may converge to the same result as other well-known methods, such as Genetic Algorithm, Particle Swarm Optimization and Cuckoo Search.* Some typical optimization results are depicted in Figs. 3 and 11, and can be found in Ref. 11, respectively. Note, this concept also includes design and generation strategies for shaping Bessel-Gaussian beams of higher orders.[11,22]

Main limitations of our method are connected to Eq. (4). The structural frequency of the transverse beam profile should be constant. Many spatial features, such as fine structure, sharp edge, large continuous area, are not available due to the absence of high and low frequency. More critical are unwanted side lopes. For example in Fig. 3 (a), the merit function is defined by a cross shape, that is summing the intensity value of the points on the cross. The resulting beam profile after the optimization, on the other hand, is not continuous and exhibits several side lopes near the cross, see Fig. 3 (b).

*Please see, for example, the documentation of MATLAB's Global Optimization Toolbox.

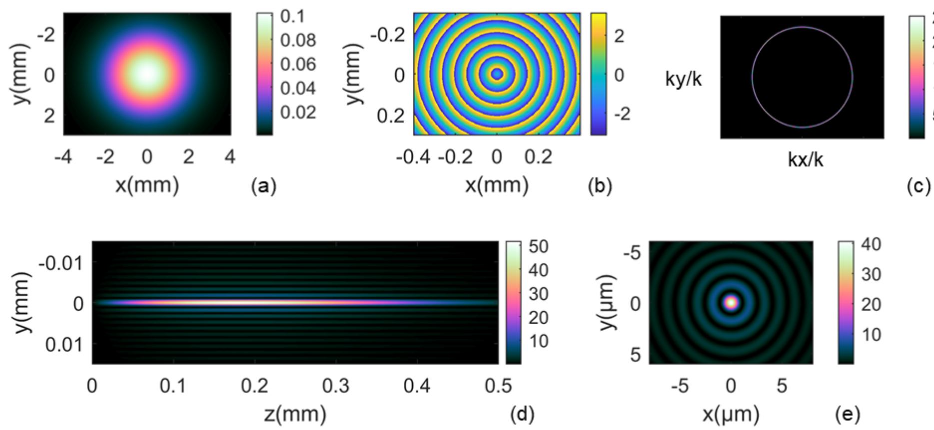

Figure 2. The simulated Bessel-like beam generated from an axicon.[1] (a) The x-y intensity profile of the Gaussian beam in arbitrary units. (b) The equivalent phase modulation of an ideal thin axicon. (c) angular spectrum of the Bessel-like beam. (d) The simulated z-y intensity profile of the Bessel-like beam (at plane $x = 0\,\text{mm}$). (e) The x-y intensity profile of the Bessel-like beam (plane $z = 0.1\,\text{mm}$).

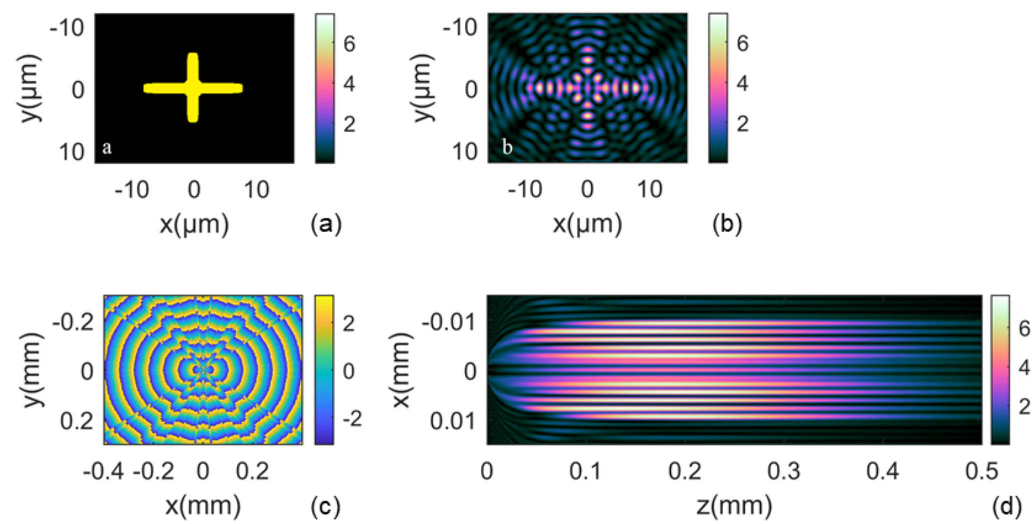

Figure 3. Comparison of the target cross-like beam profile (a) and the achieved beam profile after optimization (b).[11,23] A maximum interference contrast under the cross-like intensity envelope is clearly visible. (c) The phase mask of the cross beam (d) The longitudinal intensity profile of the cross beam.

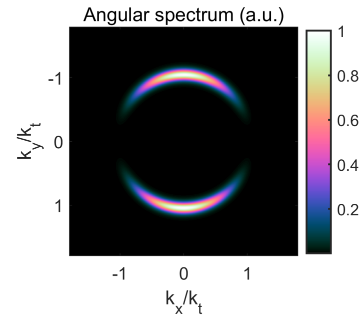

Figure 4. Angular spectrum of zeroth-order Mathieu beam.[24] With respect to the conventional Bessel-like beam, approximately $\sim 60\%$ of optical power is missing in the typical ring-like angular spectrum, cf. Fig. 2 (c).

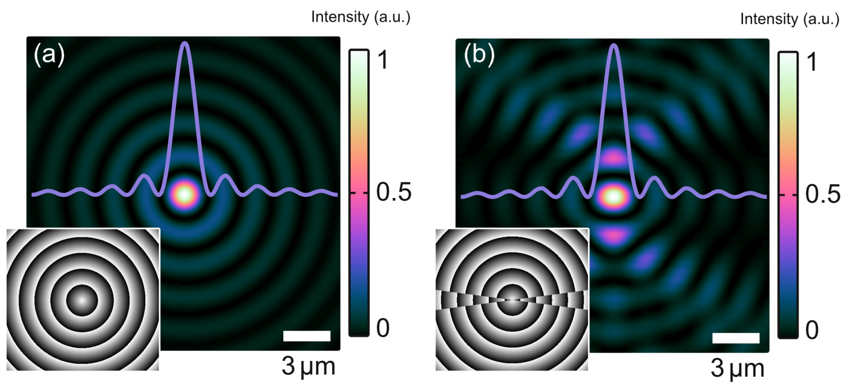

Figure 5. Near-field profile comparison of the fundamental Bessel-Gaussian beam (a), cf. Fig. 2, and one example of an elliptical non-diffracting beam generated with a generalized axicon (b). The required axicon-like phase-only holograms are depicted in the respective insets. Note, the minor modification to the phase masks (π-phase jump) that allows to control the ellipticity (orientation and main axis ratio) of the transverse beam profile.[10,11,28]

The second limitation is from the absence of amplitude modulation and the need for a phase-only beam shaping concept, respectively. Although this can ensure high energy efficiency in micro-machining application, the freedom in design is reduced. Special non-diffracting beam profiles, such as, e.g., low order Mathieu beams (propagation invariant solutions to the Helmholtz equation in elliptic cylindrical coordinates),[2,24] whose angular spectrum (squared amplitude) is different from a ring shape, see Fig. 4, are not achievable with our method.

We see the greatest strength of the generalized axicons in forming non-diffracting beams with preferential directions. The reason for this is the simplicity of the generation and the simplicity in the design of required phase holograms. Today, spatial light modulators such as digital micromirror devices[25,26] or liquid-crystal-displays[6,27] are available and affordable to everyone. The flexible generation of generalized axicons and, thus, the customized shaping of non-diffracting beams can be carried out without major constraints. In Fig. 5 the near-field profiles of the fundamental Bessel-Gaussian beam [(a), see also Fig. 2][1] can be directly compared to that of an elliptical non-diffracting beam [(b)][11,28] shaped with an axicon phase mask which is altered according to Eq. (5). For the latter, the required phase hologram (see inset) merely exhibits an additional π-phase jump in a well-defined angular segment. The impact of thus small modification seems to be minor in terms of the transverse intensity distribution and, in fact, the ratio of long to short main axis of the elliptical on-axis maximum is merely $1.5:1$. However, its impact during machining transparent materials is enormous. Please see Ref. 10 for the beneficial use of generalized axicons for facilitated glass separation. Additionally, we explicitly refer to Fig. 3 in Ref. 10 and to Fig. 2 in Ref. 11 for further design details and explanations.

As pointed out in Ref. 14 the diffractive realization of the generalized axicons is preferred in order to keep all spatial degrees of freedom. However, refractive[14] or reflective[29] version are equally feasible as well as axicon-like elements realized with geometric phase holograms.[30] The first two variants will be slightly more efficient than the diffractive axicons. Another important advantage, however, is that one does not suffer from round axicon

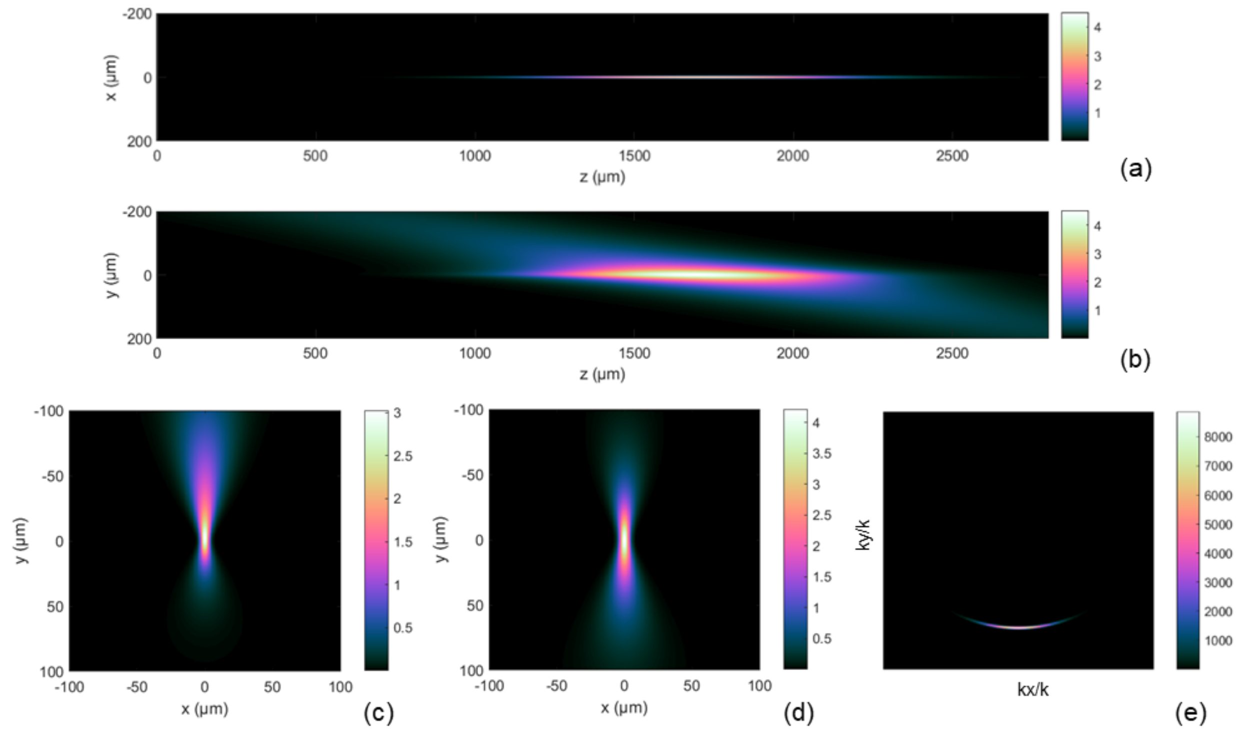

Figure 6. Intensity simulation result of the blade-like beam in arbitrary units. (a) Intensity profile in x-z plane. (b) Intensity profile in y-z plane. (c) Intensity profile in x-y plane at $z = 1400\,\mu$m. (d) Intensity profile in x-y plane at $z = 1800\,\mu$m. (e) Far-field diffraction pattern showing a ring segment.

tips[31] and that they are very reproducible in fabrication.[19]

3. NON-DIFFRACTING BEAMS WITH HIGH ASPECT RATIO

As mentioned in the previous section, one limitation of using the concept of generalized axicons is the fact that no direct amplitude modulation can be applied with the phase-only axicon-like elements.[11] A simple and feasible method for imposing amplitude modulation on the angular spectrum is changing the illumination position of the incident beam onto the axicon. Or in other words, to make use of controlled misalignments for beam shaping. This method generates a beam with blade-like shape, thus, an elongated intensity profile in longitudinal direction and a clearly elliptical transverse profile. This example, hereafter called "blade beam", is suitable for laser materials processing, especially for cutting of transparent materials.

The basic optical setup to generate the blade-like beam, see Fig. 7, is based on the widely used near-field setup for shaping Bessel-like beams using axicons, cf. Fig. 1, for cutting of transparent materials. These two systems show similar structure, complexity and robustness. The diameter of the incident Gaussian beam is, for example, 5 mm, and the angle of the used axicon may be between $(0.5 \ldots 5)$ deg . Aside from the elements shown in Fig. 7, there is a $4f$-setup to scale down the beam by a factor of $10\times$ or $20\times$ transversely and $100\times$ or $400\times$ in longitudinal direction, respectively.

In Fig. 6, an example of a blade-like beam is depicted being characterized by a high aspect ratio in both transverse direction (higher than $5:1$) and longitudinal direction (higher than $100:1$). The beam dimensions of the blade-like beam are larger than those of the fundamental Bessel-like beam under the same condition, which enables larger processing area and thus higher processing speed, but comes at the expense of higher energy demand. Under the same conditions, the simulation data of blade-like beam and Bessel-like beam are summarized in Tab. 1 for comparison. The only change in both beam shaping experiments is the illumination position of the incident Gaussian beam.

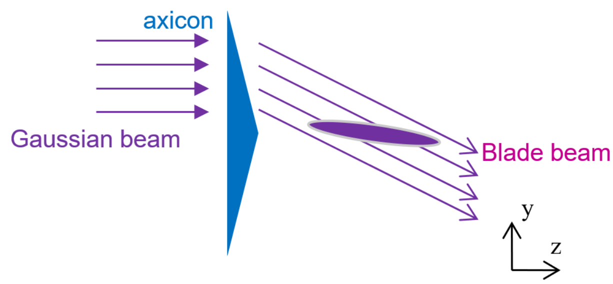

Figure 7. The basic optical setup for shaping the blade-like beam in the near-field. The fundamental Gaussian raw beam illuminates the axicon-like element with a controlled transverse spatial shift. The resulting focus distribution is imaged with a telescopic setup into the transparent workpiece.

Properties	**Bessel-like beam**	**Blade-like beam**
Illuminating position	Center of axicon	Transversely shifted
Beam size (X)	$2\,\mu$m	$(20\ldots40)\,\mu$m
Beam size (Y)	$2\,\mu$m	$5\,\mu$m
Beam size (Z)	$500\,\mu$m	$800\,\mu$m
Average Intensity	1 unit	0.1 unit
Non-diffracting beam	Yes	Yes
Far-field diffraction	Ring	Ring segment

Table 1. Comparing spatial properties of blade-like beam and Bessel-like beam.

A major benefit of the discussed concept is the ability to flexibly transform the beam profile from a conventional Bessel-like beam to the blade with extreme aspect ratios. By varying the transverse position of the incident beam, the shape and the orientation direction of the blade-like beam can be gradually controlled. When the incident beam moves around the center of axicon, the main axis directions follow this rotation. At the same time the transverse aspect ratio is controlled if the incident beam is shifted away from the optical axis defined by the axicon tip.

Theoretically, the blade-like beam is also a kind of non-diffracting beam, because its angular spectrum satisfies Eq. (4) in a very good approximation. Laser light shaped by the axicon propagates toward the z axis under the same angle. The blade beam exhibits all well-known properties of non-diffracting beams, such as self-healing and propagation invariance. However, due to limited incident beam size, the real situation slightly differs from theory, so that the resulting beam has finite size and appears tilted. Besides, the transverse profile changes gradually during propagation, see Fig. 6.

Further design options for blade-like beams can be carried out by combining the idea of generalized axicon, cf. Sec. 2, and controlled spatial misalignments, cf. Sec. 7. A menu of novel non-diffracting beam shapes can be designed and realized, see Fig. 8. Typically, these beam profiles are characterized by exploiting only a small range of the ring-like angular spectrum. In other words, if the transverse far-field intensity distribution is a short ring segment, not a complete ring, the resulting near-field focus will clearly exhibit high transverse aspect ratios.

4. MICRO-MACHINING WITH CUSTOMIZED NON-DIFFRACTING BEAMS

Possible applications of the presented beam shapes are, for example, glass cutting, selective laser etching and aberration detection as discussed in the following four sections (Secs. 4.1 − 4.4). Although our main work is on micro-machining, the generalized axicon could be used in many more cases such as optical trapping,[32] microscopy,[33] optical communication[34] etc. As mentioned in Sec. 2, we prefer the diffractive realization of generalized axicons in order to keep all spatial degrees of freedom, so that a multi-level diffractive optical element (DOE) represents a proper choice.[6] Besides, a $4f$-setup is added to the light path for scaling down the Bessel-like beam. Usually, a beam length of $\sim (0.4\ldots2)$ mm is suitable for laser glass cutting.

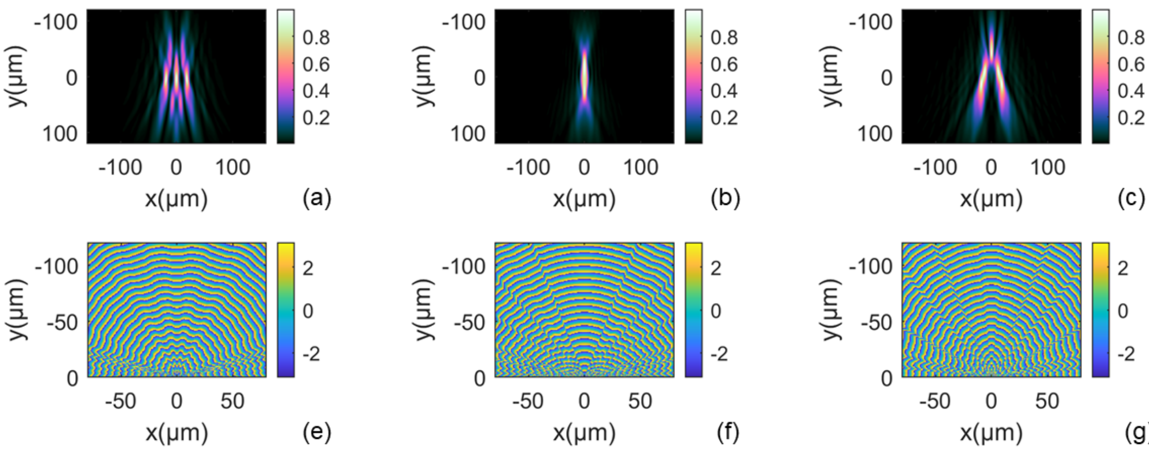

Figure 8. Menu if blade-like non-diffracting beams with customized transverse intensity profiles.(a)–(c) Transverse intensity profiles. (e)–(g) Corresponding phase masks of generalized axicons. Only the upper parts of the axicons are shown, as a transversely shifted Gaussian illumination is used.

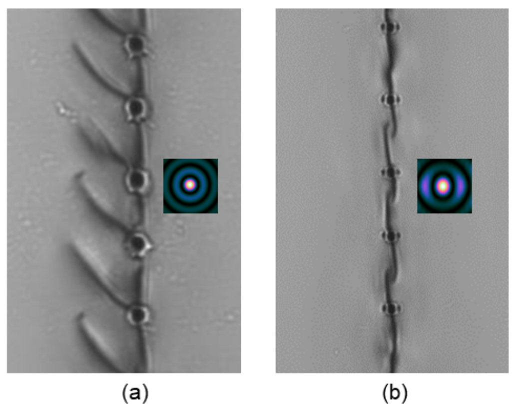

Figure 9. Processing result of conventional Bessel-like beam (a) and elliptical non-diffracting beam (b) under the same serious optical aberrations caused by the focusing unit.

4.1 Glass cutting with elliptical Bessel-like beams

Non-axisymmetric Bessel-like beams are proved to be influential to control the formation of cracks.[10,35] Tailored transverse beam profiles of non-diffracting beams can cause modifications with preferential direction reducing the necessary breaking force. Established concepts make use of spatial frequency filtering or controlled aberrations[36–38] but come at the expense of significant power loss or reduced process stability. In comparison, the generalized axicon features phase-only modulation which allows to shape elliptical Bessel beams without energy loss.

In Fig. 9, type-III-regime glass surface modifications[12] are depicted generated by a focusing unit that—by intention—imprints wave front aberrations to the shaped non-diffracting beam. The radial symmetric fundamental Bessel-like beam, see inset in (a) generates cracks that clearly do not follow the feed direction. Pulse distance (15 μm) and energy are intendedly chosen to increase visibility of this effect. Under the same optical aberrations, the elliptical Bessel-like beam [see (b)] managed to correct the orientation of cracks as the degree of ellipticity from the beam shapes dominates. So the process stability of glass cutting with preferential direction is significantly improved.

Furthermore, for some special types of glass, such as comparatively thin < 0.3 mm and thick glasses > 2 mm, the actual separation process remains challenging. In the first case, already smallest deviations from the laser induced modification layer, such as, e.g., local micro cracks, are sufficient to separate the material not along the

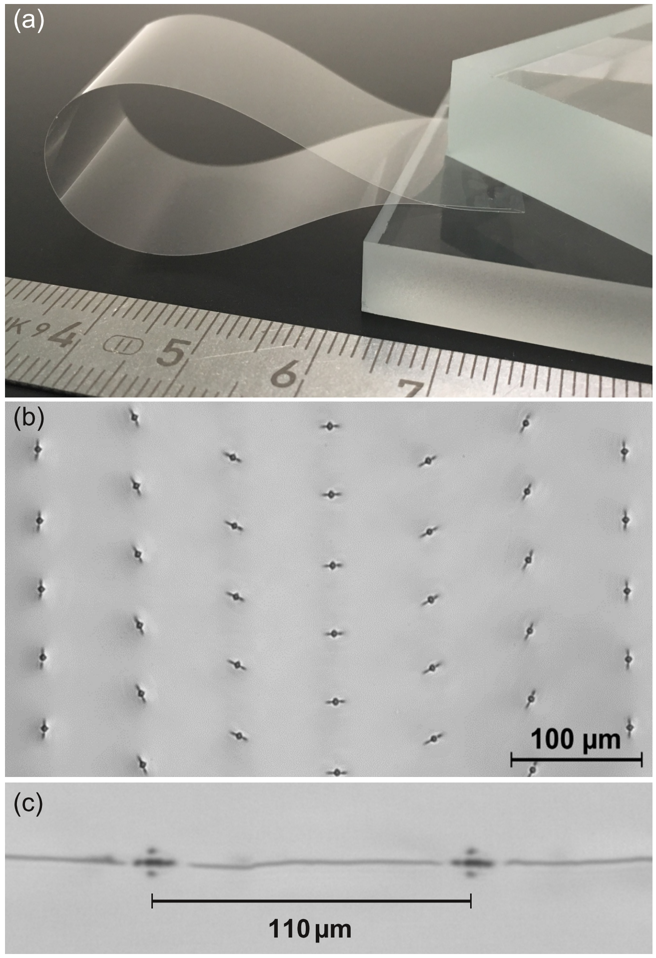

Figure 10. Processing results of facilitated separation of ultra thin (< 0.05 mm) and thick glass substrates (> 10 mm) (a). For the latter case the TOP Cleave cutting optics and a special TruMicro Series 5000 laser source providing pulse energies of 1.5 mJ was used. The orientation of cracks is controlled by rotating the central beam shaping element in 30 ° steps (b).[10,11] Modifications directly connected by cracks may well be 100 µm apart (c).[6,10]

intended contour. In the second case, for mm-scaled glass substrates, the required force necessary for separation exceeds 1 kN[10] which makes controlled cutting with high quality equally difficult.

The elliptical Bessel-like beam, with its stability and advantage in crack control, provides a promising approach to further reduce the necessary breaking force of thick glass substrates and to control the separation along predefined contours of ultra-thin glasses, respectively. More details about this facilitated glass separation concept are provided in Ref. 10. Selected processing results are depicted in Fig. 10 highlighting the successful glass cutting for two extreme glass substrate geometries.

4.2 Flower-like non-diffracting beams for aberration detection

When working with tailored non-diffracting beams, cf. Sec. 4.1, the impact of the customized beam shape, e.g., an elliptical profile, to the material process is high although the change of the transverse beam profile might be minor, cf. Fig. 9 (insets). In some cases it might be challenging to properly align the optical setup and to discriminate between intended preferential directions and induced by aberrations from misaligned optical components.[38] By choosing a well-defined non-diffracting beam that exhibits a symmetric structure and a large transverse profile, meaning that similar high intensities are distributed with large distances toward the optical axis, alignment efforts can be reduced. Such a beam profile might be the non-diffracting beam with a flower-like

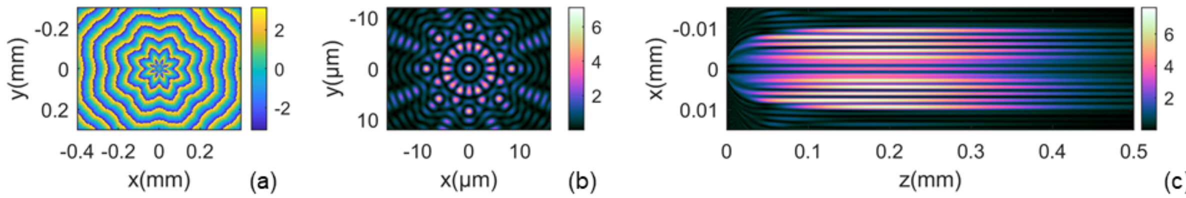

Figure 11. Generation of a flower-like non-diffracting beam (simulations). (a) The used phase mask.[11] (b) Transverse x-y intensity profile. (c) Longitudinal z-x intensity profile.[11]

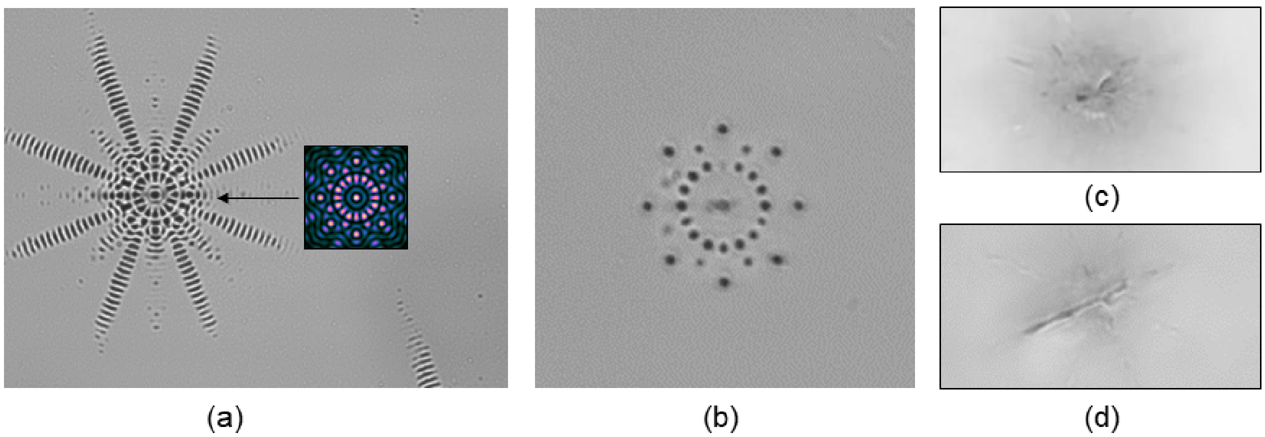

Figure 12. The flower-like beam and the corresponding processing result. Surface modifications with moderate pulse energy (a) and low pulse energy (b). Inner cracks at beam center with low aberration (c) and with strong aberration (d).

transverse intensity profile, see Fig. 11. Deviation to the ideal symmetric structure can be detected, for example, by evaluating induced surface modifications.

As a first step we consider the surface modification result depicted Fig. 12 (a) and (b) which acts as reference. If it is symmetric, the aberration is at low level. Secondly, the lopes of the flower-like beam can generate cracks that link the center beam and the side-lopes together. The focus of the microscope is set inside the glass to observe the inner cracks. Ideally if the aberration is low, the cracks are short and random, see Fig. 12 (c). If the aberration is strong then some long stable cracks appear Fig. 12 (d). This can be used to check the overall aberration of the optical setup. The alignment procedure outlined here is of high relevance if a flexible beam shaping element is used, such as the nowadays often used liquid-crystal based spatial light modulators.[6,21,39]

4.3 Glass cutting with blade-like beams

Using the optical concept shaping the discussed blade-like beam, cf. Sec. 3, we produced glass samples to discuss its beneficial use. The following laser parameters were used: Laser source: TruMicro 5070 (100 W), raw beam diameter: ~ 5 mm, pulse energy: 500 µJ in burst mode, pulse duration: 5 ps, repetition rate: 2 kHz, spatial pulse distance: (40 . . . 60) µm, glass type: Corning® Gorilla®, glass thickness: 0.33 mm.

Compared to the usage of a conventional Bessel-like beam, the pulse distance can be significantly increased to 40 µm or even more as our beam profile can be treated as an elliptical non-diffracting beam with an extreme aspect ratio.[10] The control of crack orientation is advantageous, but the surface quality, see Fig. 13, is currently inferior to the processing result of the conventional Bessel-like beam. This is due to the fact that the blade beam shows an increased focal width in the short axis of ~ 4 µm, cf. Table 1. Although we did not optimize the process yet, especially regarding transverse aspect ratio and corresponding laser parameters, we see a lot of potential with this concept. By simply off-axis shifting a standard axicon, the aspect ratio of the elliptical non-diffracting beam can be controlled. This simplicity and flexibility in combination with the gain in feed rate is an outstanding benefit.

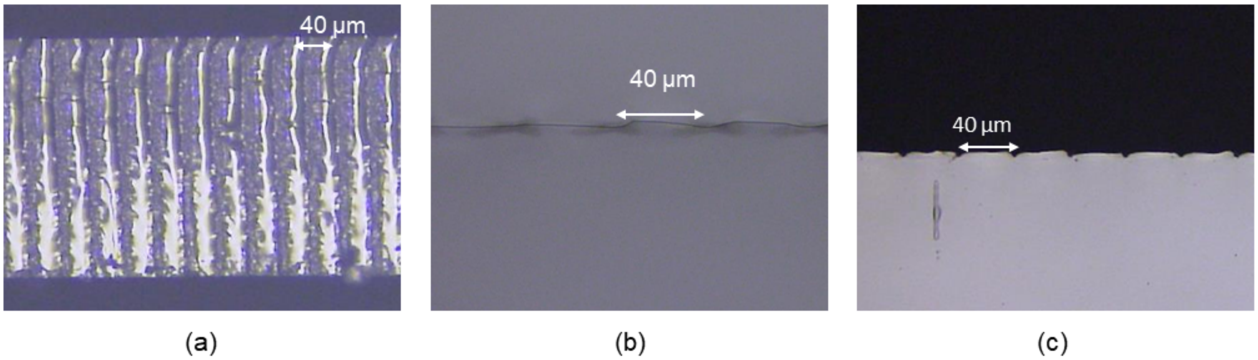

Figure 13. Microscope images of a glass sample processed with the blade-like beam. (a) The side view of edge profile after separation. (b) The top view of the processed area before separation with clearly visible crack-connected type-III-regime modifications.[12] (c) The top view of the glass edge after separation.

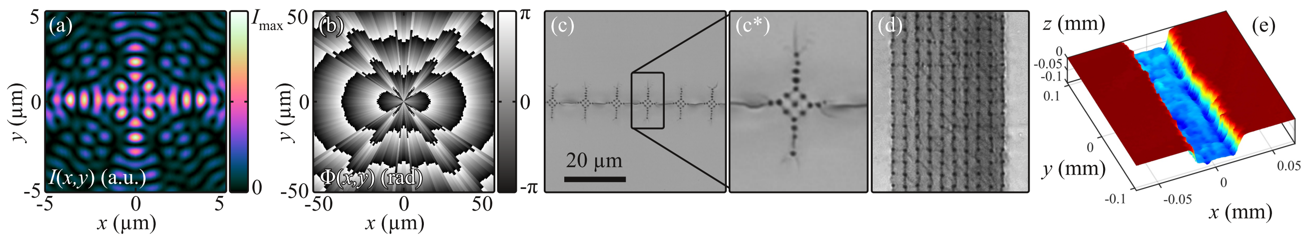

Figure 14. Efficient selective laser etching of large glass volumes based on spatial crack control. Cross-like transverse intensity profile of the nondiffracting beam (a) and phase modulation of the corresponding generalized axicon (b).[11] Microscope image of surface modifications with cross-like crack orientation (c), (c*). Plurality of surface modifications on a Cartesian grid connected by perpendicular running cracks (d). Resulting large-volume trench efficiently removed via selective etching of the crack-modified volume (e).[6,13]

4.4 Cross-like non-diffracting beams for large-volume selective laser etching

As a last example, the beneficial use of tailored non-diffracting beams for selective laser etching is demonstrated. Here, the task is to efficiently remove large volumes from glass articles. In Fig. 14 a non-diffracting beam with cross-like transverse intensity distribution is depicted, shaped by a generalized axicon,[6,13] cf. Sec. 2. Resulting volume modifications with cross-like crack orientations can be seen in (c) and (c*), respectively. A plurality of such laser-generated modifications on a Cartesian grid connected by perpendicular running cracks (d) allows to efficiently etch a large volume trench. The latter is proven by a laser scanning microscope measurement of the etched glass sample.[6,13]

5. CONCLUSION

We introduced several concepts for shaping non-diffracting beams with tailored transverse, propagation invariant intensity profiles and demonstrated their beneficial use for micro-machining of transparent materials. The concept of generalized axicons shows an enormous diversity in beam profiles useful, e.g., for facilitated glass separation or efficient selective laser etching. We discussed a theoretical model and suggested design algorithms for the optical design. In the present study, the generalized axicons were realized diffractive optically using stationary diffractive optical elements or flexible liquid-crystal-on-silicon- based spatial light modulators with achieved efficiencies above 90%.

Furthermore we discussed the concept of shaping blade-like beams using well-defined spatial misalignments of optical setups with axicons as central beam shaping elements. The concept realized with standard components enables to shape elliptical non-diffracting beams with extreme transverse aspect ratios in a simple, efficient ($\sim$ 100%) and controlled manner. This beam class was applied to cut transparent materials with large spot distances by generating crack-connected volume modifications.

We would like to point out that due to the simplicity of both the design algorithms and optical realization, we see huge potential for our concept aside from material processing, such as optical trapping and microscopy.

REFERENCES

1. D. McGloin and K. Dholakia, "Bessel beams: diffraction in a new light," *Contemporary Physics* **46**(1), pp. 15–28, 2005.
2. M. Woerdemann, *Structured Light Fields: Applications in Optical Trapping, Manipulation, and Organisation*, Springer Science & Business Media, 2012.
3. M. Bhuyan, F. Courvoisier, P. Lacourt, M. Jacquot, R. Salut, L. Furfaro, and J. Dudley, "High aspect ratio nanochannel machining using single shot femtosecond Bessel beams," *Applied Physics Letters* **97**(8), p. 081102, 2010.
4. R. Meyer, L. Froehly, R. Giust, J. Del Hoyo, L. Furfaro, C. Billet, and F. Courvoisier, "Extremely high-aspect-ratio ultrafast Bessel beam generation and stealth dicing of multi-millimeter thick glass," *Applied Physics Letters* **114**(20), p. 201105, 2019.
5. M. Jenne, F. Zimmermann, D. Flamm, D. Großmann, J. Kleiner, M. Kumkar, and S. Nolte, "Multi pulse pump-probe diagnostics for development of advanced transparent materials processing," *Journal of Laser Micro Nanoengineering* **13**(3), pp. 273–279, 2018.
6. D. Flamm, D. G. Grossmann, M. Sailer, M. Kaiser, F. Zimmermann, K. Chen, M. Jenne, J. Kleiner, J. Hellstern, C. Tillkorn, *et al.*, "Structured light for ultrafast laser micro-and nanoprocessing," *Optical Engineering* **60**(2), p. 025105, 2021.
7. H. Rave, H. Heiming, P. Szumny, M. Kaiser, J. Kleiner, and D. Flamm, "Glass tube cutting with aberration-corrected non-diffracting ultrashort laser pulses," *Optical Engineering* **60**(6), p. 065105, 2021.
8. Z. Bouchal, "Nondiffracting optical beams: physical properties, experiments, and applications," *Czechoslovak journal of physics* **53**(7), pp. 537–578, 2003.
9. D. Flamm, M. Kaiser, M. Feil, M. Kahmann, M. Lang, J. Kleiner, and T. Hesse, "Protecting the edge: Ultrafast laser modified C-shaped glass edges," *Journal of Laser Applications* **34**(1), p. 012014, 2022.
10. M. Jenne, D. Flamm, K. Chen, M. Schäfer, M. Kumkar, and S. Nolte, "Facilitated glass separation by asymmetric Bessel-like beams," *Optics Express* **28**, p. 6552–6564, 2020.
11. K. Chen, M. Jenne, D. G. Grossmann, and D. Flamm, "Generalized axicon-based generation of nondiffracting beams," *arXiv preprint arXiv:1911.03103* , 2019.
12. K. Itoh, W. Watanabe, S. Nolte, and C. B. Schaffer, "Ultrafast processes for bulk modification of transparent materials," *MRS bulletin* **31**(8), pp. 620–625, 2006.
13. M. Kaiser, M. Kumkar, R. Leute, J. Schmauch, R. Priester, J. Kleiner, M. Jenne, D. Flamm, and F. Zimmermann, "Selective etching of ultrafast laser modified sapphire," in *Laser Applications in Microelectronic and Optoelectronic Manufacturing (LAMOM) XXIV*, **10905**, p. 109050F, International Society for Optics and Photonics, 2019.
14. D. Flamm, K. Chen, M. Jenne, M. Schäfer, D. G. Grossmann, J. Hellstern, C. Tillkorn, and M. Kumkar, "Generalized non-diffracting beams for ultrafast materials processing," in *Frontiers in Ultrafast Optics: Biomedical, Scientific, and Industrial Applications XX*, **11270**, p. 112700Y, International Society for Optics and Photonics, 2020.
15. J. Durnin, "Exact solutions for nondiffracting beams. I. The scalar theory," *J. Opt. Soc. Am. A* **4**, pp. 651–654, 1987.
16. J. W. Goodman, *Introduction to Fourier Optics*, McGraw-Hill, 1996.
17. G. Indebetouw, "Nondiffracting optical fields: some remarks on their analysis and synthesis," *J. Opt. Soc. Am. A* **6**, pp. 150–152, 1989.
18. D. Flamm, J. Kleiner, M. Kaiser, F. Zimmermann, D. G. Großmann, and M. Kumkar, "Ultrafast laser cutting of transparent materials: the trend towards tailored edges and curved surfaces," in *Laser-based Micro-and Nanoprocessing XV*, **11674**, p. 116740J, International Society for Optics and Photonics, 2021.
19. D. Flamm, D. G. Grossmann, M. Jenne, F. Zimmermann, J. Kleiner, M. Kaiser, J. Hellstern, C. Tillkorn, and M. Kumkar, "Beam shaping for ultrafast materials processing," in *Laser Resonators, Microresonators, and Beam Control XXI*, **10904**, p. 109041G, International Society for Optics and Photonics, 2019.

20. U. Levy, E. Marom, and D. Mendlovic, “Thin element approximation for the analysis of blazed gratings: simplified model and validity limits,” *Optics Communications* **229**, pp. 11–21, 2004.
21. J. Leach, G. M. Gibson, M. J. Padgett, E. Esposito, G. McConnell, A. J. Wright, and J. M. Girkin, “Generation of achromatic bessel beams using a compensated spatial light modulator,” *Optics Express* **14**(12), pp. 5581–5587, 2006.
22. K. Bergner, D. Flamm, M. Jenne, M. Kumkar, A. Tünnermann, and S. Nolte, “Time-resolved tomography of ultrafast laser-matter interaction,” *Optics Express* **26**(3), pp. 2873–2883, 2018.
23. M. Kumkar, M. Kaiser, J. Kleiner, D. Grossmann, D. Flamm, K. Bergner, and S. Nolte, “Ultrafast laser processing of transparent materials supported by in-situ diagnostics,” in *Laser Applications in Microelectronic and Optoelectronic Manufacturing (LAMOM) XXI*, **9735**, p. 97350P, International Society for Optics and Photonics, 2016.
24. A. Grabusovas, V. Vosylius, T. Gertus, and S. Orlov, “Vector Mathieu beam profile engineering for laser material processing applications,” *Procedia CIRP* **74**, pp. 598–601, 2018.
25. J. Liang, R. N. Kohn Jr, M. F. Becker, and D. J. Heinzen, “High-precision laser beam shaping using a binary-amplitude spatial light modulator,” *Applied Optics* **49**(8), pp. 1323–1330, 2010.
26. J. Cheng, C. Gu, D. Zhang, and S.-C. Chen, “High-speed femtosecond laser beam shaping based on binary holography using a digital micromirror device,” *Optics Letters* **40**(21), pp. 4875–4878, 2015.
27. A. Forbes, A. Dudley, and M. McLaren, “Creation and detection of optical modes with spatial light modulators,” *Advances in Optics and Photonics* **8**(2), pp. 200–227, 2016.
28. D. Flamm and K. Chen, “Segmentiertes Strahlformungselement und Laserbearbeitungsanlage,” Oct. 21 Oct. 21 2019. DE Patent 10 2019 128 362 B3.
29. P. Boucher, J. Del Hoyo, C. Billet, O. Pinel, G. Labroille, and F. Courvoisier, “Generation of high conical angle Bessel–Gauss beams with reflective axicons,” *Applied Optics* **57**(23), pp. 6725–6728, 2018.
30. J. Kim, Y. Li, M. N. Miskiewicz, C. Oh, M. W. Kudenov, and M. J. Escuti, “Fabrication of ideal geometric-phase holograms with arbitrary wavefronts,” *Optica* **2**(11), pp. 958–964, 2015.
31. O. Brzobohatỳ, T. Čižmár, and P. Zemánek, “High quality quasi-Bessel beam generated by round-tip axicon,” *Optics Express* **16**(17), pp. 12688–12700, 2008.
32. T. Cizmar, V. Garces-Chavez, K. Dholakia, and P. Zemanek, “Optical trapping in counter-propagating bessel beams,” in *Optical Trapping and Optical Micromanipulation*, **5514**, pp. 643–651, International Society for Optics and Photonics, 2004.
33. V. Grillo, J. Harris, G. C. Gazzadi, R. Balboni, E. Mafakheri, M. R. Dennis, S. Frabboni, R. W. Boyd, and E. Karimi, “Generation and application of Bessel beams in electron microscopy,” *Ultramicroscopy* **166**, pp. 48–60, 2016.
34. N. Mphuthi, L. Gailele, I. Litvin, A. Dudley, R. Botha, and A. Forbes, “Free-space optical communication link with shape-invariant orbital angular momentum Bessel beams,” *Applied Optics* **58**(16), pp. 4258–4264, 2019.
35. R. Meyer, R. Giust, M. Jacquot, J. Dudley, and F. Courvoisier, “Submicron-quality cleaving of glass with elliptical ultrafast Bessel beams,” *Applied Physics Letters* **111**, p. 231108, 12 2017.
36. R. Meyer, M. Jacquot, R. Giust, J. Safioui, L. Rapp, L. Furfaro, P.-A. Lacourt, J. M. Dudley, and F. Courvoisier, “Single-shot ultrafast laser processing of high-aspect-ratio nanochannels using elliptical Bessel beams,” *Opt. Lett.* **42**, pp. 4307–4310, Nov 2017.
37. F. Hendricks, V. V. Matylitsky, M. Domke, and H. P. Huber, *Time-resolved study of femtosecond laser induced micro-modifications inside transparent brittle materials*, vol. 9740, SPIE, 2016.
38. J. Dudutis, R. Stonys, G. Raciukaitis, and P. Gecys, “Aberration-controlled Bessel beam processing of glass,” *Optics Express* **26**, p. 3627, 02 2018.
39. C. Rosales-Guzmán and A. Forbes, *How to shape light with spatial light modulators*, SPIE Press, 2017.